Analytical Model of Nanowire FETs in a Partially Ballistic or Dissipative Transport Regime

Paolo Michetti
Dipartimento di Ingegneria dell'Informazione: Elettronica, Informatica, Telecomunicazioni,
Università di Pisa
Giorgio Mugnaini

Giuseppe Iannaccone
Dipartimento di Ingegneria dell'Informazione: Elettronica, Informatica, Telecomunicazioni,
Università di Pisa

P. Michetti, G. Mugnaini, G. Iannaccone, *Analytical Model of Nanowire FETs in a Partially Ballistic or Dissipative Transport Regime*, IEEE Transactions on Electron Devices, **56**, 7, pp.1402-1410 (2009).

Analytical Model of Nanowire FETs in a Partially Ballistic or Dissipative Transport Regime

Paolo Michetti, Giorgio Mugnaini, and Giuseppe Iannaccone, *Member, IEEE*

***Abstract*—The intermediate transport regime in nanoscale transistors between the fully ballistic case and the quasi-equilibrium case, described by the drift-diffusion (DD) model, is still an open modeling issue. Analytical approaches to the problem have been proposed, based on the introduction of a backscattering coefficient, or numerical approaches consisting in the Monte Carlo solution of the Boltzmann transport equation or in the introduction of dissipation in quantum transport descriptions. In this paper, we propose a simple analytical model to seamlessly cover the whole range of transport regimes in generic quasi-1-D field-effect transistors, and apply it to silicon nanowire transistors. The model is based on describing a generic transistor as a chain of ballistic nanowire transistors in series, or as the series of a ballistic transistor and a DD transistor operating in the triode region. As an additional result, we find a relation between the mobility and the mean free path that has deep consequences on the understanding of transport in nanoscale devices.**

***Index Terms*—Ballistic transport, compact model, drift-diffusion (DD) transport, nanowire transistors, quantum wires, 1-D transistors.**

I. Introduction

MULTIPLE gate architectures such as gate-all-around (GAA) MOSFETs have lately attracted significant interest [1]–[3], and have emerged as promising options to keep short channel effects under control, exhibiting quasi-ideal subthreshold swing with undoped channels. This has the very important consequence of alleviating intrinsic variability of transistor threshold voltage, which in planar MOSFETs is mainly due to channel doping.

Nanowire FETs are a particular case of multiple gate FETs, in which quantum confinement occurs in the transverse cross section of only few nanometers. Nanowire FETs are basically quasi-1-D transistors, where transport occurs in a set of loosely coupled propagating modes.

From the point of view of modeling, several papers have appeared in the literature addressing transport and quantum confinement in silicon nanowire transistors (SNWTs). In pioneering works [4]–[7], the effects of quantum confinement on a silicon nanowire were discussed. Numerical detailed investigations of quantum confinement in silicon and silicon germanium nanowires with the anisotropic effective mass approximation, and its effect in lifting the degeneracy of silicon conduction band minima were discussed in [8] and [9]. The electrostatics of silicon nanowire devices with cylindrical symmetry has been investigated through a perturbative approach to the Schrödinger equation [10] or with a self-consistent solution in Poisson–Schrödinger equation with cylindrical coordinates [11].

Analytical models of ballistic nanowire transistors have been proposed in [12]–[14] and a broad review can be found in [15]. In real nanowire devices, currents are much lower than those predicted by ballistic models [2], which can only be used as an asymptotic performance limit.

Nonballistic transport in quasi-1-D channels is harder to model. As far as numerical studies are concerned, far-from-equilibrium transport in SNWTs was investigated in [16] within the nonequilibrium Green's functions formalism, for both ballistic and dissipative transport, using the Büttiker probes approach to model inelastic scattering. A subband-based drift-diffusion (DD) simulation, in which the 3-D electrostatics is solved self-consistently with the 2-D Schrödinger equation in each transverse cross section and a set of 1-D continuity equations based on the DD description, has been proposed in [17].

As far as analytical models of dissipative transport in quasi-1-D FETs are concerned, notable examples are [13], which proposed a semiclassical model with DD transport and constant mobility inside a cylindrical MOSFET, and [18], in which a polynomial expansion of the Fermi integrals for the mobile charge is used.

Specific scattering mechanisms such as phonon scattering have been numerically addressed within the nonequilibrium Green's functions approach by Jin *et al.* [19] and by Gilbert *et al.* [20], [21].

We believe that it would be very interesting to have an analytical model capable to seamlessly cover the continuum of transport regimes between the limits of ballistic transport and DD (i.e., quasi-equilibrium) transport. Such a model, theoretically derived from the formalism of Büttiker virtual probes [22], and consisting in either a chain of ballistic transistors or in the series of a fully ballistic and an ideal DD transistor, has been proposed in [23] and [24] for 2-D MOSFETs.

On the basis of this paper, we present an analytical model capable of describing the complete range of transport regimes in quasi-1-D FETs, from fully ballistic to long channel quasi-equilibrium DD behavior. A preliminary attempt has been

Manuscript received December 10, 2008; revised March 30, 2009. Current version published June 19, 2009. This work was supported in part by the EC Nanosil FP7 Network of Excellence under Contract 216171 and in part by the European Science Foundation EUROCORES Programme Fundamentals of Nanoelectronics, through fundings from Consiglio Nazionale delle Ricerche (awarded to IEEIIT-PISA) and the European Commission Sixth Framework Program under Project Dewint (Contract ERAS-CT-2003-980409). The review of this paper was arranged by Editor M. Reed.

The authors are with the Dipartimento di Ingegneria dell'Informazione, Università di Pisa, 56122 Pisa, Italy (e-mail: p.michetti@iet.unipi.it; g.inannaccone@iet.unipi.it).

Color versions of one or more of the figures in this paper are available online at http://ieeexplore.ieee.org.

Digital Object Identifier 10.1109/TED.2009.2021720

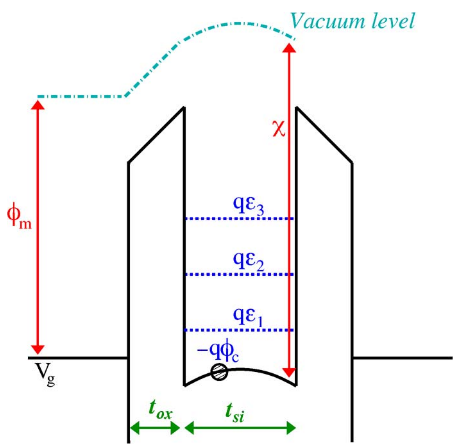

Fig. 1. Schematic band diagram of a 1-D SNWT. V_g is the gate Fermi potential, ϕ_m is the gate workfunction, χ is the channel electron affinity, ϕ_c is the potential in the centroid layer. $q\varepsilon_\alpha$ are the eigenvalues of the vertical confinement, drawn out of scale.

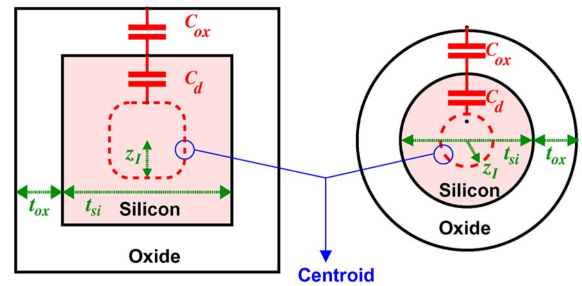

	t_{si}	t_{ox}	z_I
R	4 nm	3 nm	0.97 nm
C	4 nm	3 nm	0.92 nm

Fig. 2. Schematic capacitance diagram for a wire with square and circular cross section, representing the series of the oxide capacitance C_{ox} and the silicon capacitance C_d. In the square shape, the interface between the silicon and the insulator is considered approximately isopotential, and the mobile charge layer (the centroid z_I) is approximated with a square contour. The table summarizes the geometrical parameters used in the simulation of the rectangular wire (R) and cylindrical one (C).

proposed in [25]. As we shall show, the model is sufficiently simple to be suitable for circuit-level simulations and provides a strong intuitive picture of the transition from ballistic to DD transport, which is missing in other descriptions of partially ballistic transport such as those relying on the introduction of a backscattering coefficient [26], [27].

This paper is organized as follows: In Section II, we set up a model for ballistic transport in a nanowire transistor that, in Section III, we apply to the case of a chain of ballistic transistors. With a linearization procedure, we show that a sufficiently long chain of ballistic transistors, can be regarded as a DD channel. However, the same approach fails for short ballistic chains, in which transport has an intermediate nature between ballistic and DD. This difficulty is tackled in Section IV, where we present a compact model for intermediate transport that treats the ballistic chain as a series of one DD section, for the first $N-1$ transistors, and the remaining one ballistic channel, in which the nonequilibrium character of the intermediate transport manifests itself. In Section V, we introduce the cylindrical and rectangular confinements for silicon nanowires considered in this paper, and in Section VI, we compare the results of our DD and intermediate transport compact models with the numerical solution of the transport through ballistic chains of different length. In the section, we also give an estimation of the current ballisticity ratio as a function of the transistor chain length.

II. Ballistic Transport

In the following discussion, we describe our approach in the general situation of a n-FET with a quasi-1-D channel, with the effective mass approximation. Indeed, the subband energies are determined by the transverse confinement, and to explicitly account for the capacitive coupling between gate and channel, the contact geometry has to be taken in account. The bottom of the 1-D conduction subbands are formally defined as the sum $q\varepsilon_\alpha - q\phi_c$, of the eigenstates of the vertical confinement with respect to the conduction band edge in the centroid layer $(q\varepsilon_\alpha)$ and of the electrostatic potential energy $(-q\phi_c)$ in the centroid layer that is where one can think all charge localized, following the approach of [28] and [23] (Fig. 1). For simplicity, α denotes the set of the quantum numbers specifying the confinement. The dimensionality also modifies the Fermi–Dirac integrals $F_{\nu-1/2}$ and F_v entering the ballistic equations for the mobile charge and the current in the channel, respectively. In particular, for a 1-D conductor, in effective mass approximation, $v = 0$, whereas for a 2-D MOSFET $v = 1/2$ [24]. A definition for the Fermi integrals, with $v > -1$, is

$$F_v(\eta) = \frac{1}{\Gamma(v+1)} \int_0^\infty \frac{x^v}{e^{x-\eta}+1} dx \tag{1}$$

with Γ being the Gamma function, acting as a normalizing factor for the Fermi integrals. For $v \le -1$, we can rely to their property $(d/d\eta)F_v(\eta) = F_{v-1}(\eta)$ for their definition [29].

We start from a generic multisubband degenerate version of the ballistic model in [24]. The vertical electrostatic model we propose is similar to that in [12] and [13]; it is also somewhat less sophisticated, because we will suppose that screening can be considered constant. This is done in view of obtaining an analytical model of intermediate transport. We note that this assumption is sound enough for small cross-sectional channels and low electron densities [30]. Indeed, in the inverse layer centroid approach, we consider the charge accumulated in the centroid layer and its geometrical screening is included in the effective gate capacitance as a series contribution C_d, therefore the effective gate oxide capacitance for unit length is given by

$$C_g = \left(\frac{1}{C_{\mathrm{ox}}} + \frac{1}{C_d}\right)^{-1} \tag{2}$$

as shown in Fig. 2, where the expression C_{ox} depends on the geometry.

If we suppose an undoped channel, consistently with Fig. 1, the linear density of mobile charge on the peak of the potential barrier in the channel is given by

$$Q_m = -C_g \left[V_g - (\phi_m - \chi)/q - \phi_c\right] \tag{3}$$

where ϕ_c is the electrostatic potential in the centroid layer, $(\phi_m - \chi)/q$ is the flatband potential, given by the difference between the gate workfunction ϕ_m and the channel electron affinity χ.

In the case of ballistic transport, there is no local equilibrium so that no quasi-Fermi level can be locally defined, because two different carrier populations exist, originating from source and drain, which can be considered at equilibrium with the injecting electrodes, as discussed in [31]. These two populations are separated by the peak of the barrier in the channel that controls transport. Therefore, only three points are important: source, drain, and the peak of the electrostatic potential. In ballistic transport, carriers move without inelastic scattering along the channel and therefore at the subband peak the carriers that propagate toward the drain ("forward states") only come from the source, whereas the carriers propagating toward the source ("reverse" states) come from the drain. As a consequence, we have the superposition of two hemi-Fermi–Dirac distributions. Following the considerations in [12], we can write for the ballistic mobile charge linear density on the peak

$$Q_m = -q \sum_\alpha N_\alpha \left[F_{-1/2}\left(\eta_s^\alpha\right) + F_{-1/2}\left(\eta_d^\alpha\right)\right] \tag{4}$$

where

$$N_\alpha = g_\alpha \sqrt{\frac{k_B T m_\alpha}{2\pi^2 \hbar^2}}\,\Gamma\left(\frac{1}{2}\right)$$

is one half of the effective density of states of the αth subbands multiplied for its degeneration index g_α. $F_{-1/2}(\eta)$ is the Fermi integral of order $-1/2$ and

$$\begin{aligned}\eta_s^\alpha &= (\phi_c - V_s - \varepsilon_\alpha)/\phi_t\\ \eta_d^\alpha &= (\phi_c - V_d - \varepsilon_\alpha)/\phi_t.\end{aligned} \tag{5}$$

The Fermi potential at the source (drain) is $V_{s(d)}$ and $\phi_t = K_b T/q$ is the thermal potential. Equations (3) and (4) have to be solved simultaneously to obtain ϕ_c and Q_m.

From the Landauer formula, we can write the current as [12]

$$I_{\text{ds}} = q \sum_\alpha G_\alpha \left[F_0\left(\eta_s^\alpha\right) - F_0\left(\eta_d^\alpha\right)\right] \tag{6}$$

where $G_\alpha = g_\alpha (k_b T/\pi\hbar)\Gamma(1)$ is the effective injection rate of a 1-D channel multiplied by the degeneration g_α of the αth subband. Note that the current is dependent on the channel potential through η_s and η_d.

III. From Ballistic to DD Transport

We follow the approach developed in [23] and [24] for a 2-D MOSFET for the nondegenerate and degenerate cases. Here, we analyze the case of a SNWT where the different dimensionality leads to different Fermi integrals entering the current and the charge expressions, and to different electrostatics. Moreover, we considered a multisubband degenerate model, while in [24], only a single subband was presented. We obtain also a correcting factor for the degenerate case, correcting the result of the linearization process whenever the low field approximation is not in fully satisfied.

We recall that, within the Büttiker probes approach, inelastic scattering is thought as localized in special points, spaced by a length defined as "mean free path" λ. The virtual probes act as localized reservoirs along the channel, in which carriers are thermalized in equilibrium with their quasi-Fermi potential V_k, while transport from one virtual probe to the next is considered purely ballistic. We have a DD transistor when the channel length is much longer than the free mean path, that from our point of view, it is equivalent to have a long enough chain of ballistic transistors, as rigorously shown in [23]. On the contrary, when the number of internal contacts is small, transport is far-from-equilibrium, and is fully ballistic in the limit $N = 1$. We remark that within the Büttiker probe approach, transport of hot electrons is accounted only inside each ballistic channel, whereas a full thermalization occurs in correspondence of each probe, where electron density is described by a single quasi-Fermi level. It would also be interesting, but out of the scope of this paper, to couple the transport equation with a heat diffusion equation, accounting for the energy losses in the Büttiker probes, leading to a nonuniform temperature distribution in the device.

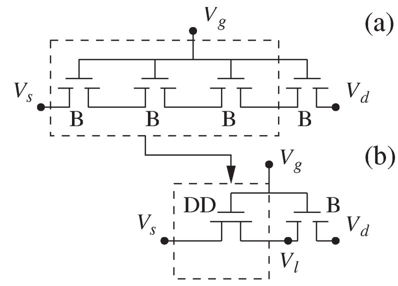

Fig. 3. (a) Circuit model of a generic SNWT, subject to inelastic scattering, in terms of a convenient chain of ballistic (B) SNWTs. (b) Approximate aggregation of the first $N-1$ ballistic transistors in an equivalent DD one. The macromodel $\mathrm{DD}+\mathrm{B}$ comes out to be a suitable model for a device in intermediate transport regime.

We define V_k as the quasi-Fermi potential of the kth virtual probe, and suppose that the kth contact is placed at $x_k = k\lambda$ with $k = 1, \ldots, N$, where the boundaries are fixed as $V_0 = V_s = 0$ V and $V_N = V_d = V_{\text{ds}}$. That is equivalent to place N ballistic SNWTs of channel length λ in series, as shown in Fig. 3. Since the current I_k in any $k = 1, \ldots, N$ FET must be equal to I_{ds}, we have N equations determining the local Fermi levels

$$I_k = q \sum_\alpha G_\alpha \left[F_0\left(\eta_{k-1}^\alpha\right) - F_0\left(\eta_k^\alpha\right)\right]. \tag{7}$$

We note that $\eta_k^\alpha = (\tilde{\phi}_k - V_k - \varepsilon_\alpha)/\phi_t$, where $\tilde{\phi}_k$ is the electrostatic self-consistent potential in the conduction band peak of channel k, between the source contact $k-1$ and the drain contact k. Introducing the definition $\tilde{V}_k \equiv (V_{k-1} + V_k)/2$, i.e., the mean potential between the two contacts (k and $k-1$) of channel k, and making explicit the Fermi integrals, we can rearrange (7) as follows:

$$I_k = q \sum_\alpha G_\alpha \int_0^\infty \frac{\sinh\left(\frac{V_k - V_{k-1}}{2\phi_t}\right)}{2\left[\cosh\left(\frac{x - \tilde{\eta}_k^\alpha}{2}\right)\right]^2 + \left[\cosh\left(\frac{V_k - V_{k-1}}{2\phi_t}\right) - 1\right]} dx \tag{8}$$

where $\tilde{\eta}_k^\alpha = (\tilde{\phi}_k - \tilde{V}_k - \varepsilon_\alpha)/\phi_t$.

At this point, in order to build an analytical model, we consider a large number of contacts and, having in mind that the current is constant along the channel, we extend V_k to a continuous quasi-Fermi potential $V(x)$ satisfying the conditions

$$V\left(\frac{x_k+x_{k-1}}{2}\right)=\tilde{V}_k \tag{9}$$

$$\frac{dV}{dx}\left(\frac{x_k+x_{k-1}}{2}\right)=\frac{V_k-V_{k-1}}{\lambda}. \tag{10}$$

Under the particular hypothesis that every ballistic SNWT works in the linear region, i.e., that

$$\lambda\frac{dV(x)}{dx}=V_k-V_{k-1}\ll 2\phi_t \tag{11}$$

and expanding the terms $\sinh$ and $\cosh$ to the first order, we can put (8) in the local form

$$I=\frac{q\lambda}{\phi_t}\frac{dV(x)}{dx}\sum_\alpha G_\alpha F_{-1}\left[\eta^\alpha(x)\right] \tag{12}$$

where the quantities pertain to all point x, as

$$\eta^\alpha(x)=\left[\phi(x)-V(x)-\varepsilon_\alpha\right]/\phi_t. \tag{13}$$

Evidently, if a voltage V_{ds} is applied to the chain, (11) is satisfied if $V_{\mathrm{ds}}\ll 2\phi_t N$. Moreover, within the same approximations, the vertical electrostatics becomes

$$Q(x)=\sum_\alpha Q^\alpha(x)=2q\sum_\alpha N_\alpha F_{-1/2}\left[\eta^\alpha(x)\right]. \tag{14}$$

An important aspect of (12) and (14) is that the current I^α in subband α can be written in terms of the mobile charge density $Q^\alpha(x)$ and of a mobility $\mu^\alpha_{\mathrm{deg}}(x)$ as

$$I^\alpha(x)=\mu^\alpha_{\mathrm{deg}}(x)Q^\alpha(x)\frac{dV(x)}{dx} \tag{15}$$

where the conduction is affected by the 1-D electron gas degeneracy through the mobility $\mu_{\mathrm{deg}}(x)$. The mobility is given by

$$\mu^\alpha_{\mathrm{deg}}(x)=\frac{v_\alpha\lambda}{2\phi_t}\frac{F_{-1}\left[\eta^\alpha(x)\right]}{F_{-1/2}\left[\eta^\alpha(x)\right]} \tag{16}$$

where $v_\alpha\lambda/2\phi_t$, to which (16) is reduced in the nondegenerate limit, represents the low-field mobility for a 1-D gas of incoming electrons described by an hemi Maxwell–Boltzmann statistics [24] occupying the αth subband, whose mean electron velocity is $v_\alpha=\sqrt{(2kT/\pi m_\alpha)}$, characterized by a ballistic motion for paths of length $l<\lambda$ and a sudden and complete scattering at $l=\lambda$. Considering the mean free path λ as a constant, (16) describes the degradation of carrier mobility due to degenerate conditions of Fermi–Dirac statistics. An analogous expression was recognized in a Monte Carlo simulation [32] for the case of strained silicon FETs. While, in [16] and [27], a similar, but not identical relation between the mean free path and the effective mobility has been found.

The current is expressed in a local form in (12), and we can eliminate the gradient of the local quasi-Fermi level integrating along the channel and exploiting current continuity, leading to

$$I_{\mathrm{ds}}=\int_0^L q\frac{\lambda}{\phi_t L}\sum_\alpha G_\alpha F_{-1}\left[\eta^\alpha(x)\right]\frac{dV(x)}{dx}dx. \tag{17}$$

In order to obtain a more compact form of (17), we can change the integral variable as follows:

$$\begin{aligned}\int_0^L qF_{-1}\left[\eta(x)\right]\frac{dV(x)}{dx}dx&=\int_{V_s}^{V_d}F_{-1}\left[\eta(V)\right]dV\\&=\int_{\eta_s}^{\eta_d}F_{-1}(\eta)\frac{dV}{d\eta}d\eta\end{aligned} \tag{18}$$

where the term $dV/d\eta$ is obtained by differentiating (14) in dV and using the fact that $d\eta/dV=(d\phi/dV-1)/\phi_t$. The current can be obtained with a numerical integration of

$$I^\alpha_{\mathrm{ds}}=\frac{q\lambda G_\alpha}{\phi_t L}\int_{V_s}^{V_d}F_{-1}\left[\eta_\alpha(V)\right]dV \tag{19}$$

where we note that η_α not only explicitly depends on V, but also implicitly through ϕ_c, as shown in (13). Such dependence has to be taken into account in the self-consistent solution of the vertical electrostatics.

Finally, we obtain the compact expression (which we will refer as the DD model) for the source–drain current for each subband α

$$\begin{aligned}I^\alpha_{\mathrm{ds}}=\frac{q\lambda\phi_t G_\alpha}{\phi_t L}\Bigg(&\left[F_0\left(\eta^\alpha_s\right)-F_0\left(\eta^\alpha_d\right)\right]\\&+\sum_\beta\rho_\beta\left[\mathcal{F}_{-1,-3/2}\left(\eta^\alpha_s,\eta^\beta_s\right)-\mathcal{F}_{-1,-3/2}\left(\eta^\alpha_d,\eta^\beta_d\right)\right]\Bigg)\end{aligned} \tag{20}$$

where, for simplicity, we defined

$$\mathcal{F}_{-1,-3/2}(\eta^\alpha,\eta^\beta)\equiv\int_{-\infty}^{\eta^\alpha}F_{-1}(x)F_{-3/2}\left(x+\frac{\varepsilon_\beta-\varepsilon_\alpha}{\phi_t}\right)dx \tag{21}$$

with $\rho_\alpha=(qN_\alpha/C_g\phi_t)$. It is worth noting that, as observed also in [23] and [24], in the nondegenerate limit the first term in (20) reduces to the diffusion term of the EKV model, while in the degenerate limit, it corresponds to the current of a single ballistic channel divided by N. The second term of (20) is instead associated with the drift current.

We note that actually, in the low field approximation, for the case of a 1-D channel, the integral (8) can be analytically solved as discussed in Appendix A. However, the use of the analytical expression leads to the more complex and numerically expensive expression for the DD current (29), while giving only a slight correction of (19). The model that employs the analytical

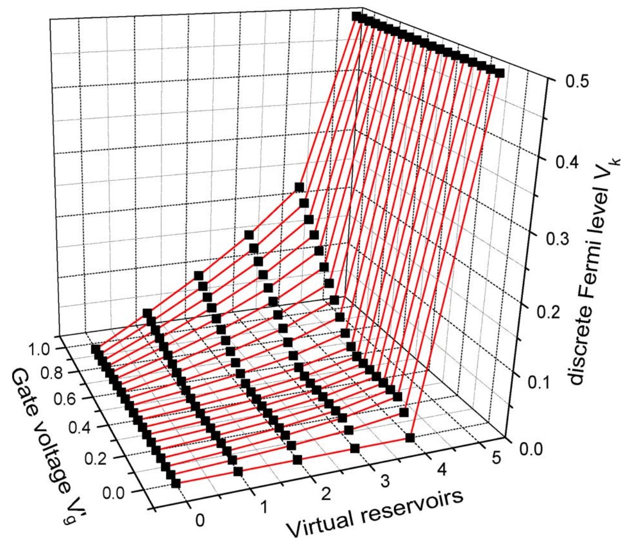

Fig. 4. Discrete quasi-Fermi potential for a chain of $N = 5$ SNWTs at fixed $V_{\rm ds} = 0.5$ V. Fermi level is defined only on the virtual probes placed at points $x = k\lambda$ with $k = 1, \ldots, N$. It is evident that the first $N - 1$ transistors work approximately in linear regime; while increasing V_g, a nonlinear behavior is developed on the latter ballistic channel. This fact supports the choice of the DD + B segmentation in our model for intermediate transport.

solution of (8), with the use of (29), will be referred as DD* model. We conclude stressing the fact that DD and DD* models, considered alone, are not appropriate to describe transport whenever the condition (11) is not satisfied: for example in very short channels, where intermediate transport is expected.

IV. Compact Model for Intermediate Transport

Now, we are interested in the development of a model that will be effective in the whole range of transport regimes, as proposed in [23] for the 2-D MOSFET case. It is evident that in the general case of intermediate transport, the simplifying hypothesis (11) that enforces each SNWT of the ballistic chain to operate in the linear region, does not hold, and we can expect that some elementary channels can work in the saturation regime, or near it [23]. The behavior of an SNWT operating in such intermediate transport regime can be obtained by solving the system for the complete ballistic chain (7), but it can represent a heavy computational burden, particularly for a large number of internal nodes. In order to build a simple model that can be more easily handled, we note in Fig. 4, where we plotted the quasi-Fermi potential on the virtual probes for a chain decomposition of an SNWT, that when the saturating behavior of the elementary ballistic transistor emerges, it is present mainly on the last ballistic transistor of the chain. This nonlinear behavior is a general condition for transistors in intermediate transport regime, due to the fact that in its end the channel narrows down and therefore, to maintain constant the current flux along it, a major spacing between the last source and drain levels is required (or, in the continuous limit, a steep drop of the quasi-Fermi level). This fact suggests that we can aggregate the first $N - 1$ ballistic transistors in an approximate equivalent DD transistor with ratio $L/\lambda = N - 1$ working in low field conditions, as it is shown in Fig. 3, and similarly to what was proposed in [23] for MOSFETs. We can therefore see an SNWT in intermediate regime as the series of a DD channel for the first $N - 1$ transistor that we can solve using (19), and a single ballistic transistor, governed by (6). We only need to solve the DD + B system, imposing constant current through the two sections in series and solving the Fermi potential on the internal node between the DD and the B channels. We point out that in the DD + B model the ratio L/λ has no need to be integer, because we apply the continuous DD equation (20).

V. Application to GAA-Silicon Nanowire

At first, we will consider a silicon wire with square cross section of side $t_{\rm si}$. Concerning the effective gate capacitance, unfortunately, no simple analytical closed form is available. In order to simplify the electrostatics, we suppose that the interface between the oxide and silicon is approximately isopotential, and we consider the variational approximation reported in [33], where the capacitance per unit length of a rectangular coaxial line, associated with the oxide layer, is

$$C_{\rm ox} = \frac{8\epsilon_{\rm ox}}{\ln\left(1 + \frac{2t_{\rm ox}}{t_{\rm si}}\right)} \tag{22}$$

and similarly the capacitance associated with the charge in the silicon body C_d is

$$C_d = \frac{8\pi\varepsilon_{\rm si}}{\ln\left(\frac{t_{\rm si}}{2z_I}\right)}. \tag{23}$$

The use of C_d, with z_I adequately chosen, permits to treat the capacitance due to the charge distribution in the channel cross section, in series with the oxide capacitance $C_{\rm ox}$. The term z_I is a characteristic radius of the closed line where we can effectively localize the whole mobile charge. Here, it is used as a fitting parameter for simplicity, while it is actually dependent, due to volume inversion, on the charge density in the channel. We point out, although, that it is smoothly varying for small section nanowires and low electron density [30].

In case of rectangular quantum confinement, the eigenvalues of the Schrödinger equation can be considered for simplicity [12]

$$q\varepsilon^{\nu}_{n_x,n_y} = \frac{\hbar^2\pi^2}{2}\left[\frac{n_x^2}{m_x^{\nu}t_{\rm si}^2} + \frac{n_y^2}{m_y^{\nu}t_{\rm si}^2}\right] \tag{24}$$

where the mass tensor can be defined as

ν	m_x^ν	m_y^ν	m_z^ν
1	m_t	m_l	m_t
2	m_l	m_t	m_t
3	m_t	m_t	m_l

m_l and m_t are the longitudinal and transverse components of the effective mass tensor of the degenerate minima of the conduction bands in Si. We can write the effective mass, characterizing the motion in the unconfined direction (z), as $m_\alpha = m_z^\nu$ for a (100) silicon wire, with ν running on the different Si conduction band minima.

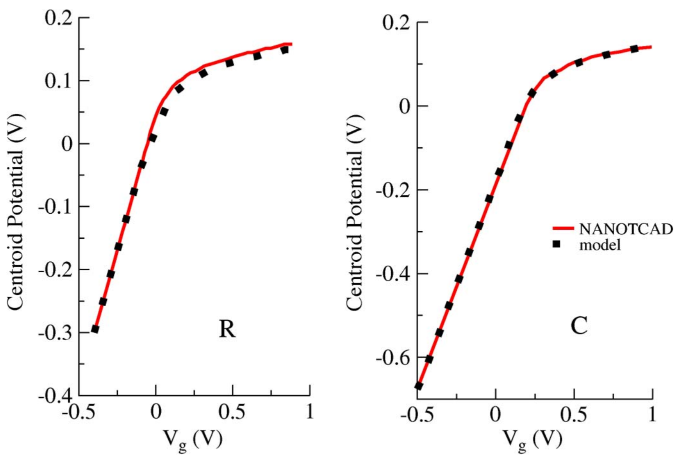

Fig. 5. Comparison between NANOTCAD 2-D simulation and the compact model calculation of the vertical electrostatic for the R and C SNWTs. The centroid potential obtained with (solid line) NANOTCAD 2-D and the centroid potential obtained with the (dotted) compact model are reported. The compact model well accounts for the centroid potential, point in which the charge of the channel can thought to be concentrated.

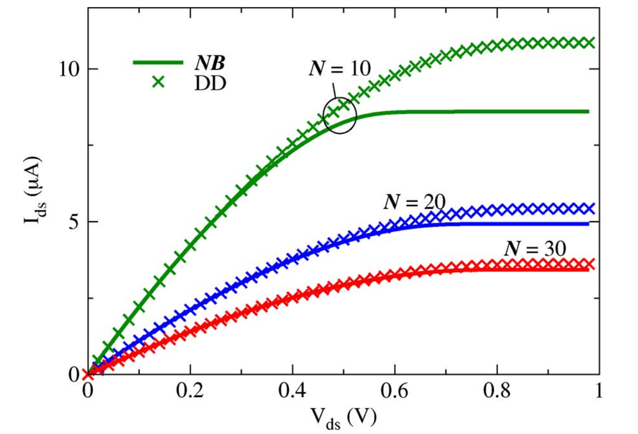

Fig. 6. Output characteristics for a chain of N ballistic cylindrical C SNWTs (denoted by NB), for N = 10, 20, 30, compared with results of the DD model with $\lambda = L/N$. The gate potential value is $V_g = 0.8$ V. As the number of ballistic transistors in series increases, the DD approximation become more and more able to capture the behavior of the device.

In the case of cylindrical quantum confinement, for the gate capacitance, we have instead

$$C_{\text{ox}} = \frac{2\pi\varepsilon_{\text{ox}}}{\ln\left(1+\frac{2t_{\text{ox}}}{t_{\text{si}}}\right)} \tag{25}$$

$$C_d = \frac{2\pi\varepsilon_{\text{si}}}{\ln\left(\frac{t_{\text{si}}}{2z_I}\right)}. \tag{26}$$

Considering cylindrical quantum confinement [12], we have that the subband separation from the bottom of the conduction band is described by the approximated and handy expression

$$q\varepsilon^{\nu}_{n_1,n_2} \simeq \frac{\hbar^2\pi^2}{2\sqrt{m^{\nu}_x m^{\nu}_y}R^2}\left(n_1+|n_2|-\frac{1}{4}\right)^2 \tag{27}$$

where n_1 is the radial quantum number, n_2 the azimuthal quantum number, and ν runs on the different silicon valleys.

We applied our model to a cylindrical quantum wire and a rectangular SNWT, denominated C, R, respectively. Their geometries are shown in Fig. 2. The inversion centroid layer depth was fixed in comparison with the 2-D Schrödinger–Poisson simulator NANOTCAD [34], as shown in Fig. 5. We note that a careful choice of z_I permits to recover the inverse layer centroid potential in full agreement with the NANOTCAD simulator, correctly accounting, thus, for the screening due to the charge inside the channel as a function of the gate potential.

VI. Results

For a short channel transistor with length of few mean free paths, transport is quasi-ballistic, and we have seen that the DD model (19) fails to describe its behavior. On the other hand, it is well known that the transport regime of a transistor with channel length much longer than the free mean path is described by the DD model. We want to check if our model is able to correctly reproduce such transition and to investigate the number of free mean paths after which transport can be definitely associated to the DD regime. In Fig. 6, we plot the output characteristics for a chain of N ballistic channels numerically calculated (denoted NB) and with the DD approximation (DD characteristics), for N = 10, 20, 30 and gate potential $V_g = 0.8$ V. We note that for an SNWT of length smaller than 10 λ, a DD description is not appropriate. With increasing N, the difference between the NB and DD models is reduced, and for a channel of length $> 20\lambda$, the output characteristics calculated with the DD model fully reproduce the corresponding numerically evaluated NBs.

We have calculated the output characteristics of SWNTs described in the latter section employing a direct numerical solution of the chain of N ballistic transistors (NB), and compared them with our models for intermediate transport DD + B and DD* + B. Figs. 7 and 8, respectively, show the output characteristics for the C SWNT with $N = L/\lambda = 5$, and for the rectangular SWNT with $N = 2$. Similar considerations apply to the two figures. While the DD approximated equation, derived from the linearization of the NB chain, inadequately reproduces the saturation behavior of the NB characteristics, the DD + B model seems suitable to describe SNWTs in the intermediate transport regime. As shown in Figs. 7 and 8, the DD + B and DD* + B models are really able to capture the nonlinear behavior of the NB transistors, although a non-negligible error remains in the saturation regime. This is due to the weakly nonlinear transport in the DD section that has been neglected. We note that, in general, the DD* + B improves the agreement with the ballistic chain characteristics.

After testing our model with rectangular and cylindrical nanowire geometries, changing both the oxide and silicon length t_{ox}, t_{si} and with different values of N, we can conclude that the DD + B and DD* + B compact model quite well reproduces the output characteristics of degenerate SWNTs for any N, with errors in the saturation zone of few percentage points.

In Fig. 9, the transfer characteristics of a C SNWT, treated as a chain of N elementary ballistic channels, with $V_{\text{ds}} = 0.5$ V, is presented. Both the DD + B and the DD* + B models well

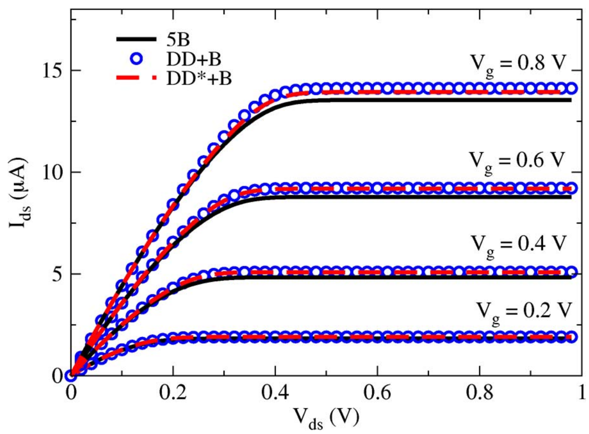

Fig. 7. Output characteristics of a C SNWT modeled as a chain of $N = 5$ elementary transistors: 5B corresponds to the exact numerical evaluation. The $\mathrm{DD} + \mathrm{B}$ compact model is obtained considering the series of a DD channel governed by (20) plus a ballistic one and the $\mathrm{DD}^* + \mathrm{B}$ is analogous but uses (29) for the DD section. The choices of the gate potential are $V_g = 0.2$, 0.4, 0.6, and 0.8 V.

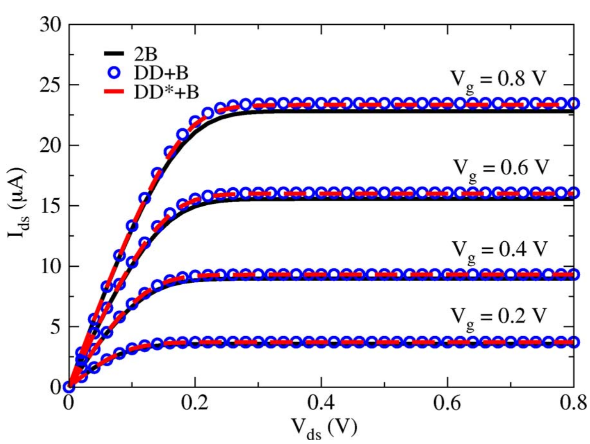

Fig. 8. Output characteristics of the R SNWT modeled as a chain of $N = 2$ elementary transistors: exact numerical evaluation (2B), compact model $\mathrm{DD} + \mathrm{B}$ with a DD plus a ballistic channels and $\mathrm{DD}^* + \mathrm{B}$ analogous to the latter except for the use of (29) in the DD section. The choices of the gate potential are $V_g = 0.2$, 0.4, 0.6, and 0.8 V.

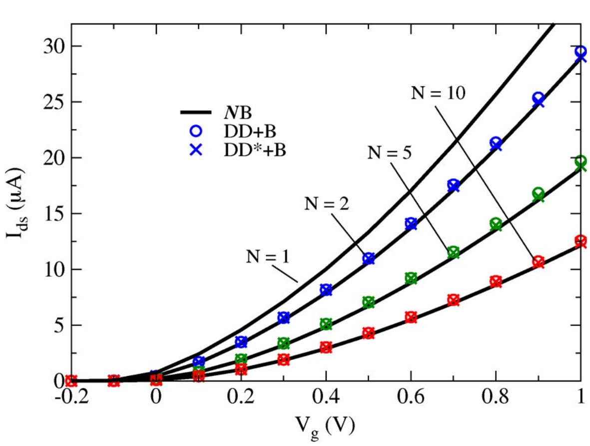

Fig. 9. Transcharacteristic curves for a chain of N ballistic C SNWTs, with N ranging from 1 to 10 and $V_{\mathrm{ds}} = 0.5$ V. The exact numerical evaluation (NB), and the results of the $\mathrm{DD} + \mathrm{B}$ and $\mathrm{DD}^* + \mathrm{B}$ compact models are shown.

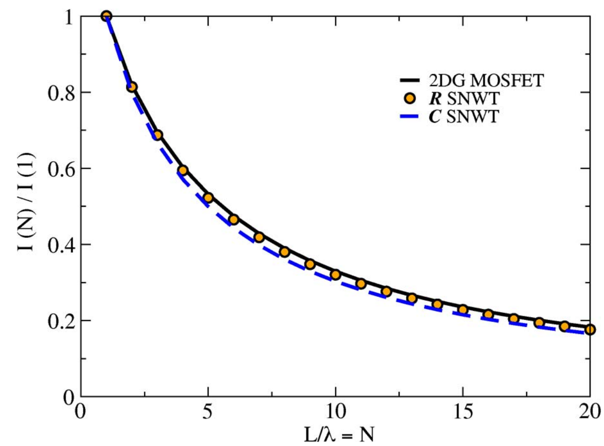

Fig. 10. Ballisticity index of a NB chain as a function of N for the R, C SNWTs, and a MOSFET (see text for details). The gate potential is $V_g = 0.8$ V, and the drain-source potential is $V_{\mathrm{ds}} = 0.5$ V.

reproduce the behavior of the corresponding ballistic chain in all gate voltage regimes, for all values of N. We note that the $\mathrm{DD}^* + \mathrm{B}$ model is always more accurate, in particular the correction is more evident for transistor with few nodes, at large gate voltage.

We investigated also the so-called ballisticity index of a transistor [35] that is given by the current ratio I/I_b, between the current of the transistor and that of a corresponding ballistic one. The results of its calculation for a NB chain, with N ranging from 1 to 20, are shown in Fig. 10, where we considered the R, C SNWTs and also, for comparison an undoped Double Gate MOSFET with $t_{\mathrm{si}} = 4$ nm, $t_{\mathrm{ox}} = 2$ nm. The ballisticity index is monotonous and slowly decaying with N, the behavior is similar for all the transistors considered here. The curves can be easily fitted with the function $1/[1 + r(N - 1)]$, where N is the number of ballistic elements and $r \approx 0.25$. We note that initially the ballisticity index steeply decreases with N. For longer channels, the current becomes slowly varying with N: sliding from $N = 10$ to $N = 20$ the current only decreases from the 30% to the 20% of the ideal ballistic one.

Having in mind a compact model, the calculation of equations (20) or (19) for the $\mathrm{DD} + \mathrm{B}$ model are still computationally expensive. Therefore, we also tested the approximation of the integral in the DD section (DD) with its symmetrical linearization [36], as discussed in Appendix B.

VII. Conclusion

We have presented a physics-based analytical model able to describe quasi-1-D field-effect transistors in the complete range of transport regimes extending from the fully ballistic case captured by the Natori model to the quasi-equilibrium case captured by the DD description. Our proposed model sees a generic transistor as a long enough chain of elementary ballistic transistors in series with a common gate. Based on the Büttiker probes description of inelastic scattering, we have rigorously proved that the model reduces to the limit cases. In addition, as the most important result in this paper, we have shown that an equally adequate model, much simpler from the computational point of view, and more physically intuitive, is represented by the series of an appropriate DD 1-D transistor and a ballistic 1-D transistor, consistently with the results in [23] and [24] that apply to 2-DEG FETs. We have focused in this paper on SNWTs, but our model is applicable without significant variations to any type of quasi-1-D FET, such as those based on carbon nanotubes, graphene nanoribbons, or other channel materials.

Finally, we have shown that an interesting consequence of our model is that, if a uniformly spaced chain is assumed, the Fermi–Dirac statistics degrades the low-field mobility, consistently with the observations in [32].

APPENDIX A
ANALYTICAL SOLUTION OF THE DD INTEGRAL

We note that in the integral

$$\int_0^\infty \frac{1}{2\left[\cosh\left(\frac{x-\tilde{\eta}^\alpha}{2}\right)\right]^2+\left[\cosh\left(\frac{V_k-V_{k-1}}{2\phi_t}\right)-1\right]}dx$$

in (8) has an analytical solution given by

$$\mathcal{I}(\tilde{\eta}) = \frac{1}{\sqrt{a(a+1)}} \times\left\{\tanh^{-1}\left[\sqrt{\frac{a}{a+1}}\right]+\tanh^{-1}\left[\sqrt{\frac{a}{a+1}}\tanh\left(\frac{\tilde{\eta}^\alpha}{2}\right)\right]\right\}$$

where $a=[\cosh((V_k-V_{k-1}/2\phi_t))-1]/2$. We replace the Fermi level difference between neighbor probes, by its mean value on the linearized chain

$$V_k - V_{k-1} \approx \gamma = \Delta V^{(\mathrm{DD})}/(2\phi_t N)$$

where $\Delta V^{(\mathrm{DD})}$ is the total potential drop in the DD section and N the number of elementary channels in it.

In the low-field approximation, we also replaced the $\sinh((V_k-V_{k-1}/2\phi_t))$ with its arguments: We try to amend this by including a correction factor obtained by the ratio of the not-approximate term over approximate one

$$\sinh\left(\frac{V_k-V_{k-1}}{2\phi_t}\right)\Big/\frac{V_k-V_{k-1}}{2\phi_t}. \tag{28}$$

In the end, we reach a more accurate version of (19) for the DD section, given by the following expression:

$$I^\alpha = \frac{q\lambda G_\alpha}{\phi_t L}\frac{\sinh(\gamma)}{\gamma\sqrt{a(a+1)}}\int_{V_s}^{V_d}\mathcal{I}[V]dV. \tag{29}$$

APPENDIX B
SYMMETRICAL LINEARIZATION OF THE DD INTEGRAL IN SNWT

The integral for the DD current (19) is computationally expensive for a compact model to be included in circuit simulators such as SPICE. Therefore, we adopt a variant of the symmetrical linearization [36], [37] in order to obtain an approximated result

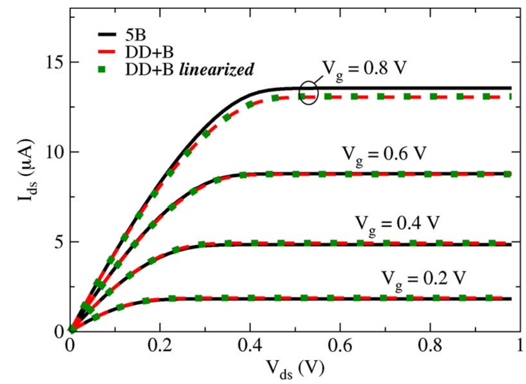

Fig. 11. Characteristic curves calculated for a R SNWT with $N=5$. The results of the direct numerical calculation 5B, of the $\mathrm{DD}+\mathrm{B}$ compact model and of the same compact model, employing symmetrical linearization $\mathrm{DD_{lin}}+\mathrm{B}$, discussed in the text, are shown. The curves are calculated for gate potential values of $V_g=0.2$, 0.4, 0.6, and 0.8 V.

$$\begin{aligned} I &= \int_{V_s}^{V_d} q\sum_\alpha G_\alpha F_{-1}\left(\frac{\phi_c - V - \varepsilon_\alpha}{\phi_t}\right)\frac{dV}{dx}\frac{\lambda}{L}dx \\ &= \int_{\phi_{\mathrm{cs}}}^{\phi_{\mathrm{cd}}} q\sum_\alpha G_\alpha F_{-1}\left(\frac{\phi_c - V - \varepsilon_\alpha}{\phi_t}\right)\frac{dV}{d\phi_c}\frac{\lambda}{L}d\phi_c \\ &\simeq q\sum_\alpha G_\alpha F_{-1}\left(\frac{\phi_{c,m} - V - \varepsilon_\alpha}{\phi_t}\right)\left(\frac{dV}{d\phi_c}\right)_m\frac{\lambda}{L}[\phi_{\mathrm{cd}}-\phi_{\mathrm{cs}}] \\ &\simeq q\frac{\lambda}{L}\sum_\alpha G_\alpha F_{-1}\left(\frac{\phi_{c,m} - V - \varepsilon_\alpha}{\phi_t}\right)[\phi_{\mathrm{cd}}-\phi_{\mathrm{cs}}]n_q \end{aligned}$$

where we have defined the "quantum slope factor"

$$n_q \equiv 1 + \frac{1}{q\sum_\alpha \rho_\alpha F_{-\frac{3}{2}}\left(\frac{\phi_{c,m}-V_{c,m}-\varepsilon_\alpha}{\phi_t}\right)} \tag{30}$$

that is a constant in the considered case. The linearization is done around

$$\phi_{c,m} = \frac{\phi_{\mathrm{cs}}+\phi_{\mathrm{cd}}}{2} \tag{31}$$

where ϕ_{cs} and ϕ_{cd} can be obtained solving the vertical electrostatics (14). Moreover, from vertical electrostatics we find $V_{c,m}$ with an iterative process. We can observe in Fig. 11 that the symmetrical linearization of the DD integral well reproduce the not-approximated results.

REFERENCES

[1] L. Lauhon, M. Gudiksen, D. Wang, and C. Lieber, "Epitaxial core-shell and core-multishell nanowire heterostructures," *Nature*, vol. 420, no. 6911, pp. 57–61, Nov. 2002.

[2] N. Singh, A. Agarwal, L. Bera, T. Liow, R. Yang, S. Rustagi, C. Tung, R. Kumar, G. Lo, N. Balasubramanian, and D. Kwong, "High-performance fully depleted silicon nanowire (diameter $\leq$ 5 nm) gate-all-around CMOS devices," *IEEE Electron Device Lett.*, vol. 27, no. 5, pp. 383–386, May 2006.

[3] S. Suk, K. Yeo, K. Cho, M. Li, Y. Yeoh, S. Lee, S. Kim, E. Yoon, M. Kim, C. Oh, S. Kim, D. Kim, and D. Park, "High-performance twin silicon nanowire MOSFET (TSNWFET) on bulk Si wafer," *IEEE Trans. Nanotechnol.*, vol. 7, no. 2, pp. 181–184, Mar. 2008.

[4] G. Sanders, C. Stanton, and Y. Chang, "Theory of transport in silicon quantum wires," *Phys. Rev. B, Condens. Matter*, vol. 48, no. 15, pp. 11 067–11 076, Oct. 1993.

[5] M. Shen and S. Zhang, "Band gap of a silicon quantum wire," *Phys. Lett. A*, vol. 176, no. 3/4, pp. 254–258, May 1993.

[6] X. Baie, J. Colinge, V. Bayot, and E. Grivei, "Quantum-wire effects in thin and narrow SOI MOSFETs," in *Proc. IEEE Int. SOI Conf.*, Oct. 1995, pp. 66–67.

[7] J. Colinge, X. Baie, V. Bayot, and E. Grivei, "A silicon-on-insulator quantum wire," *Solid State Electron.*, vol. 39, no. 1, pp. 49–51, Jan. 1996.

[8] G. Curatola and G. Iannaccone, "Quantum confinement in silicon-germanium electron waveguides," *Nanotechnology*, vol. 13, no. 3, pp. 267–273, May 2002.

[9] A. Trellakis and U. Ravaioli, "Directional effects on bound states for trench oxide quantum wires (100)-silicon," *Solid State Electron.*, vol. 48, no. 3, pp. 367–371, Mar. 2004.

[10] E. Gnani, S. Reggiani, M. Rudan, and G. Baccarani, "A new approach to the self-consistent solution of the Schrödinger–Poisson equations in nanowire MOSFETs," in *ESSDERC*, Sep. 2004, pp. 177–180.

[11] E. Pokatilov, V. Fomin, S. Balaban, V. Gladilin, S. Klimin, J. Devreese, W. Magnus, W. Schoenmaker, N. Collaert, M. V. Rossum, and K. D. Meyer, "Distribution of fields and charge carriers in cylindrical nanosize silicon-based metal–oxide–semiconductor structures," *J. Appl. Phys.*, vol. 85, no. 9, pp. 6625–6631, May 1999.

[12] D. Jiménez, J. Sáenz, B. Iniguez, J. Suné, L. Marsal, and J. Pallarès, "Unified compact model for the ballistic quantum wire and quantum well metal–oxide–semiconductor field-effect-transistor," *J. Appl. Phys.*, vol. 94, no. 2, pp. 1061–1068, Jul. 2003.

[13] D. Jiménez, B. Iniguez, J. Suné, L. Marsal, J. Pallarès, J. Roig, and D. Flores, "Continuous analytic *I–V* model for surrounding-gate MOSFETs," *IEEE Electron Device Lett.*, vol. 25, no. 8, pp. 571–573, Aug. 2004.

[14] B. Iniguez, D. Jimenez, J. Roig, H. Hamid, L. Marsal, and J. Pallares, "Explicit continuous model for long-channel undoped surrounding gate MOSFETs," *IEEE Trans. Electron Devices*, vol. 52, no. 8, pp. 1868–1873, Aug. 2005.

[15] B. Iniguez, T. Fjeldly, A. Lazaro, F. Danneville, and M. Deen, "Compact-modeling solutions for nanoscale double-gate and gate-all-around MOSFETs," *IEEE Trans. Electron Devices*, vol. 53, no. 9, pp. 2128–2141, Sep. 2006.

[16] J. Wang, E. Polizzi, and M. Lundstrom, "A three-dimensional quantum simulation of silicon nanowire transistors," *J. Appl. Phys.*, vol. 96, no. 4, pp. 2192–2203, Aug. 2004.

[17] G. Fiori and G. Iannaccone, "Three-dimensional simulation of one-dimensional transport in silicon nanowire transistors," *IEEE Trans. Nanotechnol.*, vol. 6, no. 8, pp. 524–529, Sep. 2007.

[18] B. Paul, R. Tu, S. Fujita, M. Okajima, T. Lee, and Y. Nishi, "Theory of ballistic nanotransistors," *IEEE Trans. Electron Devices*, vol. 54, no. 7, pp. 1637–1644, Jul. 2007.

[19] S. Jin, Y. Park, and H. S. Min, "A three-dimensional simulation of quantum transport in silicon nanowire transistor in presence of electron-phonon interactions," *J. Appl. Phys.*, vol. 99, no. 12, p. 123 719, Jun. 2006.

[20] M. Gilbert, R. Akis, and D. Ferry, "Phonon-assisted ballistic to diffusive crossover in silicon nanowire transistor," *J. Appl. Phys.*, vol. 98, no. 9, p. 094 303, Nov. 2005.

[21] M. Gilbert and S. Banerjee, "Ballistic to diffusive crossover in III–IV nanowire transistors," *IEEE Trans. Electron Devices*, vol. 54, no. 4, pp. 645–653, Apr. 2007.

[22] M. Büttiker, "Role of quantum coherence in series resistors," *Phys. Rev. B, Condens. Matter*, vol. 33, no. 5, pp. 3020–3026, Mar. 1986.

[23] G. Mugnaini and G. Iannaccone, "Physics-based compact models of nanoscale MOSFETs—Part I: Transition from drift-diffusion to ballistic transport," *IEEE Trans. Electron Devices*, vol. 52, no. 8, pp. 1795–1801, Aug. 2005.

[24] G. Mugnaini and G. Iannaccone, "Physics-based compact models of nanoscale MOSFETs—Part II: Effects of degeneracy on transport," *IEEE Trans. Electron Devices*, vol. 52, no. 8, pp. 1802–1806, Aug. 2005.

[25] G. Mugnaini and G. Iannaccone, "Analytical model for nanowire and nanotube transistor covering both dissipative and ballistic transport," in *Solid-State Device Res. Conf.*, Sep. 2005, pp. 213–216.

[26] M. Lundstrom, "Elementary scattering theory of the Si MOSFET," *IEEE Electron Device Lett.*, vol. 18, no. 7, pp. 361–363, Jul. 1997.

[27] A. Rahman and M. Lundstrom, "A compact scattering model for the nanoscale double-gate MOSFET," *IEEE Trans. Electron Devices*, vol. 49, no. 3, pp. 481–489, Mar. 2002.

[28] J. Lopez-Villanueva, P. Cartujo-Cassinello, F. Gamiz, J. Banqueri, and A. Palma, "Effects of the inversion layer centroid on the performance of double-gate MOSFETs," *IEEE Trans. Electron Devices*, vol. 47, no. 1, pp. 141–146, Jan. 2000.

[29] M. Goano, "Algorithm 745: Computation of the complete and incomplete Fermi–Dirac integral," *ACM Trans. Math. Softw.*, vol. 21, no. 3, pp. 221–232, Sep. 1995.

[30] J. Roldan, A. Godoy, F. Gamiz, and M. Balaguer, "Modeling the centroid and the inversion charge in cylindrical surrounding gate MOSFETs, including quantum effects," *IEEE Trans. Electron Devices*, vol. 55, no. 1, pp. 411–416, Jan. 2008.

[31] C. Crowell and M. Hafizi, "Current transport over parabolic potential barriers in semiconductor devices," *IEEE Trans. Electron Devices*, vol. 35, no. 7, pp. 1087–1095, Jul. 1988.

[32] J. Watling, L. Yang, M. Borici, R. Wilkins, A. Asenov, J. Barker, and S. Roy, "The impact of interface roughness scattering and degeneracy in relaxed and strained Si n-channel MOSFETs," *Solid State Electron.*, vol. 48, no. 8, pp. 1337–1346, Aug. 2004.

[33] C. Liang, X. Shi, and J. Yang, "The variational closed-form formulae for the capacitance of one type of conformal coaxial lines," *Prog. Electromagn. Res.*, vol. 45, pp. 277–289, 2004.

[34] G. Curatola and G. Iannaccone, "NANOTCAD2D: Two-dimensional code for the simulation of nanoelectronic devices and structures," *Comput. Mater. Sci.*, vol. 28, no. 7, pp. 342–352, Jul. 2003.

[35] K. Natori, "Ballistic/quasi-ballistic transport in nanoscale transistor," *Appl. Surf. Sci.*, vol. 254, no. 19, pp. 6194–6198, Jul. 2008.

[36] T. L. Chen and G. Gildenblat, "Symmetric bulk charge linearisation in charge-sheet MOSFET model," *Electron. Lett.*, vol. 37, no. 12, pp. 791–793, Jun. 2001.

[37] X. Gu and G. Gildenblat, "Charge-sheet MOSFET model with surface degeneracy and freezeout," in *Int. Semicond. Device Res. Symp.*, Dec. 2001, pp. 102–105.

Paolo Michetti received the M.S. degree in material science and the Ph.D. degree in physics from the Università di Pisa, Pisa, Italy, in 2004 and 2008, respectively. His Ph.D. was devoted to theoretical investigation of the optical properties of organic nanostructured materials, like J-aggregate microcavities in strong light-matter coupling regime, in particular focusing on the effects of disorder and the modeling of their photoexcitation dynamics.

He is currently with the Dipartimento di Ingegneria dell'Informazione, Università di Pisa, as a Postdoc for a research activity on modeling and simulation of nanoelectronic devices, based on nanowires, nanotubes, and graphene nanoribbons.

Giorgio Mugnaini received the M.S.E.E. and Ph.D. degrees from the "Università di Pisa," Pisa, Italy, in 2003 and 2005, respectively.

During his Ph.D. study, from 2004 to 2005, he investigated compact modeling of intermediate transport between ballistic to drift-diffusion regimes. During 2006, he was involved in testing and development of software for railway purposes. From the fall of 2006 to present, he is employed in GIS software development. He is currently with the Dipartimento di Ingegneria dell'Informazione, Università di Pisa.

Giuseppe Iannaccone (M'98) received the M.S.E.E. and Ph.D. degrees in electrical engineering from the "Università di Pisa," Pisa, Italy, in 1992 and 1996, respectively.

Since 1996, he has been with the Dipartimento di Ingegneria dell'Informazione, Università di Pisa, first as an Assistant Professor and, since January 2001, as Associate Professor of electronics. He has coordinated a few European and National Projects involving multiple partners, and has acted as Principal Investigator in several research projects funded by public agencies at the European and National level, and by private organizations. He has authored and coauthored more than 120 papers published in peer-reviewed journals which have received more than 850 citations, and more than 80 papers in proceedings of international conferences. He is in the technical committee of few international conferences and serves as a referee for the leading journals in the fields of condensed matter physics, device electronics, and circuit design. His interests include transport and noise in nanoelectronic and mesoscopic devices, development of device modeling and TCAD tools, and the design of extremely low-power circuits and systems for RFID and ambient intelligence scenarios.